J|A|C|S ARTICLES

Published on Web 08/26/2009

Structure and Dynamics of Monomer−Template Complexation: An Explanation for Molecularly Imprinted Polymer Recognition Site Heterogeneity

Björn C. G. Karlsson,[†] John O'Mahony,[†] Jesper G. Karlsson,[†] Helen Bengtsson,[†] Leif A. Eriksson,[‡] and Ian A. Nicholls*,[†]

Bioorganic and Biophysical Chemistry Laboratory, School of Pure and Applied Natural Sciences, University of Kalmar, SE-391 82 Kalmar, Sweden and School of Chemistry, National University of Ireland — Galway, Galway, Ireland

Received March 17, 2009; E-mail: Ian.Nicholls@hik.se

Abstract: We here present the first simulation of a complete molecularly imprinted polymer prepolymerization system. Molecular dynamics studies were performed for a system comprising a total of 1199 discrete molecules, replicating the components and concentrations employed in the corresponding polymer synthesis. The observed interactions correlate well with results obtained from ^{1}H NMR spectroscopic studies. Comparison with simulations performed in the absence of cross-linking agent (ethylene dimethacrylate) demonstrated its significance in the formation of ligand recognition sites. Moreover, the influence of events such as template−template (bupivacaine) and monomer−monomer (methacrylic acid) self-association, porogen−template interactions, and template conformational variability was revealed. The template recognition capacity of the modeled polymer system was verified by synthesis of imprinted and reference polymers and subsequent radioligand binding analysis. Collectively, through a series of statistical analyses of molecular trajectories in conjunction with spectroscopic data it was demonstrated that an ensemble of complex structures is present in the prepolymerization mixture and that this diversity is the basis for the binding site heterogeneity observed in molecularly imprinted polymers (MIPs) prepared using the noncovalent strategy.

Introduction

Molecular imprinting has become a widely used method for creating ligand-specific polymeric materials with recognition properties analogous to biomolecular systems.[1] A crucial step in the preparation of these materials lies in the self-assembly of functional monomer−template complexes prior to polymerization. Formation of these complexes has been investigated using spectroscopic and theoretical approaches.[2−6] Spectroscopic data permit evaluation of the nature and number of interactions formed and represent an average of the ensemble of complexes present in solution. In contrast, theoretical methods, generally based on quantum mechanical treatments, allow for the modeling of intermolecular interactions using static structures in low-energy conformations. Nonetheless, to date, neither technique has been able to account for the binding-site heterogeneity frequently observed in the final polymer products.[7] A number of factors have been proposed to contribute to heterogeneity, including temperature,[8] incomplete template complexation, and self-association of both template structures and functional monomers. These phenomena have been reported for several

[†] University of Kalmar.
[‡] National University of Ireland.

(1) (a) *Molecularly Imprinted Polymer-Man made Mimics of Antibodies and Their Applications in Analytical Chemistry*; Sellergren, B., Ed.; Elsevier: Amsterdam, 2001. (b) *Molecularly Imprinted Materials—Sensors and Other Devices*; Shea, K. J., Roberts, M. J., Yan, M., Eds.; MRS Proceedings 723; Materials Research Society: Warrendale, PA, 2002. (c) *Molecularly Imprinted Materials: Science and Technology*; Yan, M., Ramström, O., Eds.; Dekker: New York, 2005. (d) *Molecular Imprinting: From Fundamentals to Applications*; Komiyama, M., Ed.; Wiley-VCH: Weinheim, 2002. (e) Haupt, K.; Mosbach, K. *Chem. Rev.* **2000**, *100*, 2495–2504. (f) Wulff, G. *Chem. Rev.* **2002**, *102*, 1–27. (g) Alexander, C.; Andersson, H. S.; Andersson, L. I.; Ansell, R. J.; Kirsch, N.; Nicholls, I. A.; O'Mahony, J.; Whitcombe, M. J. *J. Mol. Recognit.* **2006**, *19*, 106–180.

(2) (a) Andersson, H. S.; Nicholls, I. A. *Bioorg. Chem.* **1997**, *25*, 203–211. (b) Svenson, J.; Andersson, H. S.; Piletsky, S. A.; Nicholls, I. A. *J. Mol. Recognit.* **1998**, *11*, 83–86.

(3) (a) Sellergren, B.; Lepistö, M.; Mosbach, K. *J. Am. Chem. Soc.* **1988**, *110*, 5853–5860. (b) Whitcombe, M. J.; Martin, L.; Vulfson, E. N. *Chromatographia* **1998**, *47* (7/8), 457–464.

(4) (a) Subrahmanyam, S.; Piletsky, S. A.; Piletska, E. V.; Chen, B.; Karim, K.; Turner, A. P. F. *Biosens. Bioelectron.* **2001**, *16*, 631–637. (b) Chianella, I.; Karim, K.; Piletska, E. V.; Preston, C.; Piletsky, S. A. *Anal. Chim. Acta* **2006**, *559*, 73–78. (c) Piletsky, S. A.; Karim, K.; Piletska, E. V.; Day, C. J.; Freebairn, K. W.; Legge, C.; Turner, A. P. F. *Analyst* **2001**, *126*, 1826–1830. (d) Chianella, I.; Lotierzo, M.; Piletsky, S. A.; Tothill, I. E.; Chen, B.; Karim, K.; Turner, A. P. F. *Anal. Chem.* **2002**, *74* (6), 1288–1293.

(5) Maier, N. M.; Buttinger, G.; Welharitizki, S.; Gavioli, E.; Lindner, W. *J. Chromatogr. B* **2004**, *804*, 103–111.

(6) Diñeiro, Y.; Menéndez, M. I.; Blanco-López, M. C.; Lobo-Castañón, M. J.; Miranda-Ordieres, A. J.; Tuñón-Blanco, P. *Anal. Chem.* **2005**, *77*, 6741–6746.

(7) Szabelski, P.; Kaczmarski, K.; Cavazzini, A.; Chen, Y.-B.; Sellergren, B.; Guiochon, G. *J. Chromatogr. A* **2002**, *964*, 99–111.

(8) (a) Mijangos, I.; Navarro-Villoslada, F.; Guerreiro, A.; Piletska, E.; Chianella, I.; Karim, K.; Turner, A.; Piletsky, S. *Biosens. Bioelectron.* **2006**, *22*, 381–387. (b) O'Shannessy, D. J.; Ekberg, B.; Mosbach, K. *Anal. Biochem.* **1989**, *177*, 144–149. (c) Nicholls, I. A. *J. Mol. Recognit.* **1998**, *11*, 79–82. (d) Piletsky, S. A.; Guerreiro, A.; Piletska, E. V.; Chianella, I.; Karim, K.; Turner, A. P. F. *Macromolecules* **2004**, *37*, 5018–5022.

10.1021/ja902087t CCC: $40.75

systems, in particular in nonaqueous media in which solvent-dependent template (and monomer) self-association has been shown to influence polymer performance, as seen in the cases of nicotine,[9,10] quercetin,[11] and naproxen.[12] Despite this, in typical theoretical analyses of prepolymerization solutions, the influence of explicit solvent, multiple molecules of template, functional and cross-linking monomers, and initiator on the nature, number, and dynamics of the noncovalent interactions underlying template complexation are generally not considered. Recently, Henthorn and Peppas examined the influence of the cross-linking density of a MIP on its recognition characteristics through simulation of the prepolymerization step.[13]

We recently reported a preliminary investigation of the applicability of molecular dynamics (MD) to noncovalent MIP systems, demonstrating correlations between NMR data and MD simulations of the prepolymerization mixture.[12] It was apparent that models for the interaction of functional monomers and templates based upon more than one of each species are necessary to describe complexation and thus ultimately predict polymer behavior. In the present study, a comprehensive theoretical analysis of the various intermolecular interactions present in a prepolymerization mixture was undertaken and results were correlated with complexation studies performed using ^{1}H NMR spectroscopy. Further, the nature of the observed structure and dynamics of the prepolymerization mixture was compared and contrasted with polymer−ligand recognition behavior, as determined by radioligand binding studies. A mixture incorporating the template bupivacaine, methacrylic acid (MAA), ethylene dimethacrylate (EDMA), and 2,2′-azobis-(isobutyronitrile) (AIBN) in chloroform was simulated. Chloroform was chosen as porogen on account of its extensive use in molecular imprinting protocols and due to the availability of the well-parametrized chloroform model present in the AMBER 8 suite of programs. The bupivacaine molecular imprinting system was chosen for study due to the extensive number of previous studies using this template.[14−19]

Collectively, through the use of MD simulations employing multiple templates, functional monomers and cross-linking monomers in explicit solvent, a description of the prepolymerization mixture was obtained which correlates well with ^{1}H NMR spectroscopic studies. Statistical treatments of the MD data revealed an ensemble of template complexes, which we propose are the basis for the heterogeneity of the binding site populations observed in bupivacaine MIPs.

Experimental Section

Chemicals. Racemic bupivacaine was obtained by partitioning of (*R*,*S*)-bupivacaine-hydrochloride (Sigma, >99%) between basic brine and CH_2Cl_2. [^{3}H]-(*R*,*S*)-bupivacaine (specific activity 2.6 Ci/mmol) was from Moravek Biochemicals Inc.; EDMA (100 mL, Fluka, ≥97%) was extracted three times with a mixture of aqueous NaOH (0.1 M, 75 mL) and saturated NaCl (25 mL) and then once with saturated NaCl solution (25 mL) to remove inhibitors. The washed EDMA was dried over magnesium sulfate and stored in a freezer under nitrogen. EDMA was filtered through aluminum oxide prior to use, MAA (Sigma) was distilled under reduced pressure, and AIBN (Janssen Chimica) was recrystallized from methanol. Isobutyric acid (99%) was purchased from Alfa Aesar. Acetic-acid-d_4 (99.9 atom-% D) and chloroform-*d* (99.8 atom-% D, stabilized with 0.5 wt % silver foil, containing 0.03% v/v TMS) were obtained from Aldrich. All solvents used were of analytical grade and used as received.

^{1}H NMR Spectroscopy. All experiments were performed on NMR spectrometers operating at either 250 (Bruker AC-250) or 500 (Varian Unity Inova) MHz at 298 ± 1 K using chloroform-*d* as solvent. Apparent binding constants and statistical data were determined using a nonlinear one-site binding model implemented in the GraphPad Prism analysis software (v. 4.0, GraphPad, USA).

Titration Experiments. MAA-Bupivacaine. Aliquots of a stock solution containing 2.36 M MAA and 34 mM bupivacaine were added to an NMR tube containing 0.5 mL of 34 mM of bupivacaine. Changes in the chemical shifts, $\Delta\delta$ (ppm), of selected bupivacaine and MAA protons were determined and plotted as a function of the concentration of MAA added (4.71 mM to 1.35 M).

Acetic-Acid-d_4-Bupivacaine in the Presence of EDMA. A similar experiment was performed as described above, though in the presence of a constant concentration of EDMA (1.87 M). This concentration of EDMA was chosen in order to mimic the polymerization conditions employed during the syntheses of bupivacaine-imprinted polymer systems having a template−cross-linker molar ratio of 1:55 using toluene as the porogen.[16]

EDMA-Bupivacaine. As a control experiment, a 34 mM solution of bupivacaine was titrated with consecutive additions of EDMA (7.6 mM to 1.2 M), maintaining a constant concentration of bupivacaine throughout the whole experiment. The changes in the chemical shifts, $\Delta\delta$ (ppm), of both bupivacaine and EDMA protons were studied upon increasing the concentration of EDMA.

MAA-Bupivacaine Continuous Variation Study. Two stock solutions of MAA and bupivacaine (each 34 mM) were mixed in 10 different NMR tubes maintaining a total concentration of bupivacaine and MAA of 34 mM in each tube. The mole fractions examined for either the template or the functional monomer were in the range of 0.1−1.0. The mole fraction of bupivacaine, f_T, was subsequently plotted versus the product, $\Delta\delta \times f_T$ (Job plot).

Polymer Gelation. A mixture of bupivacaine, MAA, EDMA (molar ratio 1:12:55), and AIBN (1.3 mol % of the total amount of polymerizable methacrylate units) in chloroform-*d* (1.6 × volume of the monomers) was prepared and analyzed using ^{1}H NMR spectroscopy before and after UV irradiation at 365 nm. Spectra were recorded after 1, 3, 6, 10, 15, 30, and 45 min of irradiation and after the sample had been cooled on ice to inhibit the polymerization process.

Polymer Synthesis and Evaluation. Polymer Preparation. A bupivacaine molecularly imprinted polymer, MIP, was prepared according to a protocol previously described[14] however using chloroform as porogen instead of toluene. Racemic bupivacaine (0.35 mmol), MAA (4.2 mmol), EDMA (19 mmol), and AIBN (0.53 mmol) were weighed into a glass reaction vial and dissolved in chloroform (6.3 mL). The polymerization mixture was initially sparged with nitrogen for 15 min on ice before being placed under a UV source (365 nm) at 281 K for 24 h. The resultant bulk polymer

(9) Svenson, J.; Karlsson, J. G.; Nicholls, I. A. *J. Chromatogr. A* **2004**, *1024*, 39–44.
(10) Andersson, H. S.; Karlsson, J. G.; Piletsky, S. A.; Koch-Schmidt, A. C.; Mosbach, K.; Nicholls, I. A. *J. Chromatogr. A* **1999**, *848*, 39–49.
(11) O'Mahony, J.; Wei, S.; Molinelli, A.; Mizaikoff, B. *Anal. Chem.* **2006**, *78*, 6187–6190.
(12) O'Mahony, J.; Karlsson, B. C. G.; Mizaikoff, B.; Nicholls, I. A. *Analyst* **2007**, *132*, 1161–1168.
(13) Henthorn, D. B.; Peppas, N. A. *Ind. Eng. Chem. Res.* **2007**, *46* (19), 6084–6091.
(14) Andersson, L. I. *Analyst* **2000**, *125*, 1515–1517.
(15) Rosengren, A. M.; Karlsson, J. G.; Andersson, P. O.; Nicholls, I. A. *Anal. Chem.* **2005**, *77*, 5700–5705.
(16) Karlsson, J. G.; Andersson, L. I.; Nicholls, I. A. *Anal. Chim. Acta* **2001**, *435*, 57–64.
(17) Karlsson, J. G.; Karlsson, B.; Andersson, L. I.; Nicholls, I. A. *Analyst* **2004**, *129*, 456–462.
(18) Courtois, J.; Fischer, G.; Sellergren, B.; Irgum, K. *J. Chromatogr. A* **2006**, *1109*, 92–99.
(19) Courtois, J.; Fischer, G.; Schauff, S.; Albert, K.; Irgum, K. *Anal. Chem.* **2006**, *78* (2), 580–584.

was manually ground and sieved, and polymer particles ≤ 50 μm in diameter were collected after removing fine particles through repeated sedimentation from acetone (5 × 200 mL). After a rigorous washing procedure,[17] polymer particles were subsequently dried (313 K for 24 h) and finally stored in a desiccator until used. A nonimprinted reference polymer (REF) was prepared identically though in the absence of template. Dry polymer surface areas were characterized by BET analysis (Department of Chemical Engineering, University of Lund, Sweden).

Radioligand Binding Studies. A constant amount of radiolabeled bupivacaine (4.36 ng) was mixed with increasing concentrations of polymer (0−10 mg/mL) in a total volume of 1.0 mL using toluene instead of chloroform as the rebinding medium at 298 K in 1.5 mL Eppendorf tubes (chloroform is an efficient quencher and interferes with the scintillation counting process). After incubation for 3 h on a rocking table, the tubes were centrifuged at 10 000*g* for 5 min. After this treatment, 600 μL of the supernatant was removed from the samples, mixed with 2.0 mL of scintillation cocktail *(*Beckman Ready Safe), and finally measured by liquid scintillation counting for 2 min. (Packard Tri-Carb 2100TR liquid scintillation counter). The amount of bupivacaine bound (B) to the polymers is presented as the ratio B/T, where T is the total amount of bupivacaine accessible for binding in the bupivacaine−polymer mixtures. Specific binding to the bupivacaine molecularly imprinted polymers was calculated as the difference $(B/T)_{MIP} - (B/T)_{REF}$ for every polymer concentration studied. All binding data are presented as the result from triplicate experiments as mean ± standard error of the mean.

Molecular Dynamics (MD) Simulations. Prepolymerization Solutions. All simulations were performed using the AMBER (v. 8.0, UCSF, San Francisco, CA) suite of programs.[20] The molecular systems studied were built and parametrized using the Amber99[21] and GAFF[22] force fields. Partial atomic charges were assigned using the AM1-BCC charge method[23] within the ANTECHAMBER program. Initially, mixtures were energy minimized to remove bad van der Waals contacts using 5000 steepest-descent and 5000 conjugate gradient steps. After these energy minimization procedures, the systems were heated from 0 to 293 K at constant volume prior to an isothermal equilibration step at constant pressure (293 K and 1 bar) to ensure that the system evolved to achieve a stable density and energy. Finally, statistical data were extracted from these equilibrated NPT systems during a 5 ns production phase under conditions of NVT.

In these simulations, periodic boundary conditions were employed together with a 10 Å nonbonded interaction cutoff treating long-range electrostatics using the particle mesh Ewald (PME) summation method.[24,25] Long-range van der Waals interactions in the system were treated using a continuum model correction to energy and pressure. Temperature and pressure were kept constant using Langevin dynamics with a collisional frequency of 1.0 ps^{-1} and isotropic positional scaling with a pressure time relaxation of 2.0 ps, respectively. All hydrogen atoms in the system were constrained using the SHAKE algorithm allowing a time step of 0.002 ps (see Tables S1 and S2 (Supporting Information) for further details regarding system design and methodology). Final production phase trajectories were analyzed using the PTRAJ module implemented in AMBER, typically saving data every 0.2 ps.

Chart 1. Atoms Studied Using Radial Distribution Functions (RDFs) and Hydrogen Bond analysis

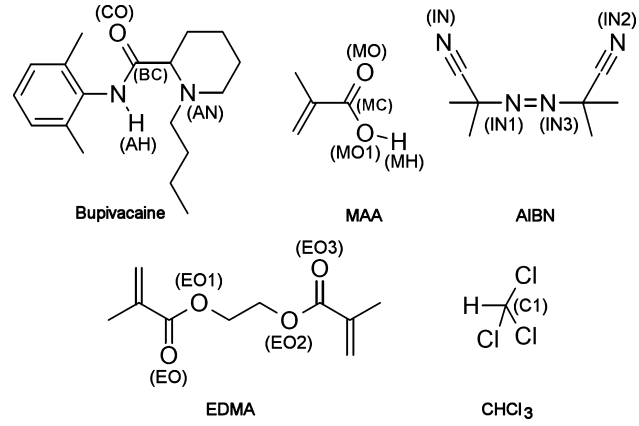

Radial distribution functions (RDFs) were generated to quantify local densities of specified atom pairs (Chart 1) at the optimal distance for interaction ($r_{opt.}$). In these analyses, the radial distribution function, $g(r)$, is defined as the ratio between the observed number density, ρ_{ij}, of a specified solvent atom at a certain distance (r) from a solute atom (i) and the average bulk atom number density of the solvent, $\langle\rho_j\rangle$. Additionally, the radial shell number, $n_{ij}(r)$, is the binned number of atoms in a volume fragment, V_{shell}, which is dependent on the bin width used, δr according to eq 1.

$$g(r) = \frac{\rho_{ij}(r)}{<\rho_j>} = \frac{n_{ij}(r)}{<\rho_j>4\pi r^2\delta r} \quad (1)$$

Grid density representations were created according to a method described by Jitera and Kollman[26] using the *grid* command in PTRAJ. With this command, boxes (100 × 100 × 120 grid points using a cubic grid cell spacing of 0.5 Å × 0.5 Å × 0.5 Å/grid point) were centered on each of the seven individual bupivacaine molecules (time-averaged, low root-mean-square deviation conformations) in each of the systems studied. All grid illustrations are presented at a contour level of either 30 (≥6 ps) or 300 (≥60 ps). Molecular graphics images were produced using the UCSF Chimera package from the Resource for Biocomputing, Visualization, and Informatics at the University of California, San Francisco (supported by NIH P41 RR-01081).[27]

To keep track of all hydrogen bond interactions formed during the MD simulations, the analysis tool *hbond* was utilized to measure all interactions taking place in solution between specified hydrogen bond donating and accepting atoms on bupivacaine, MAA, or EDMA. In this screening process, all interactions were extracted from the trajectory data using a bond cutoff distance of 3.0 Å and an angle cutoff of 60°.

Variations in bupivacaine α and β dihedral angles (defined in Chart 2) throughout simulations were studied to investigate the influence on these angles due to template complexation.

Potentials of Mean Force (PMFs). Prior to the generation of potentials of mean force (PMFs),[28] which were performed using an umbrella sampling methodology, mixtures were designed and setup as described in the previous section. Potentials for the noncovalent interactions formed between MAA and bupivacaine were calculated for systems comprised of 1 molecule of MAA, 1 molecule of bupivacaine, and 184 molecules of chloroform. Each series of simulations was performed using an additional harmonic-restraint imposed potential, $V'(d)$, on the distance (d) between one

(20) Case, D. A.; Cheatham, T. E., III.; Darden, T.; Gohlke, H.; Luo, R.; Merz, K. M., Jr.; Onufriev, A.; Simmerling, C.; Wang, B.; Woods, R. J. *J. Comput. Chem.* **2005**, *26*, 1668–1688.
(21) Wang, J.; Cieplak, P.; Kollman, P A. *J. Comput. Chem.* **2000**, *21*, 1049–1074.
(22) Wang, J.; Wolf, R. M.; Caldwell, J. W.; Kollman, P. A.; Case, D. A. *J. Comput. Chem.* **2004**, *25*, 1157–1174.
(23) Jakalian, A.; Jack, D. B.; Bayly, C. I. *J. Comput. Chem.* **2002**, *23*, 1623–1641.
(24) Essmann, U.; Perera, L.; Berkowitz, M. L.; Darden, T.; Lee, H.; Pedersen, L. G. *J. Chem. Phys.* **1995**, *103*, 8577–8593.
(25) Cheatham, T. E., III.; Miller, J. L.; Fox, T.; Darden, T. A.; Kollman, P. A. *J. Am. Chem. Soc.* **1995**, *117*, 4193–4194.
(26) Pitera, J.; Kollman, P. *J. Mol. Graph. Model.* **1997**, *15*, 355–358.
(27) Pettersen, E. F.; Goddard, T. D.; Huang, C. C.; Couch, G. S.; Greenblatt, D. M.; Meng, E. C.; Ferrin, T. E. *J. Comput. Chem.* **2004**, *25* (13), 1605–1612.
(28) Roux, B. *Comput. Phys. Commun.* **1995**, *91*, 275–282.

Chart 2. Template Molecule Studied[a]

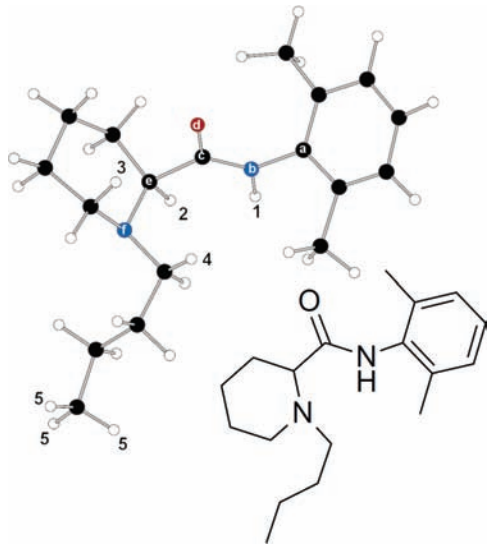

[a] The local anaesthetic drug, bupivacaine. Protons studied by ^{1}H NMR spectroscopy are numbered 1−5, and heavy atoms defining the two dihedral angles, studied by MD, are described by the greek letters α (atom a → b → c → d) and β (atoms d → c → e → f).

atom on bupivacaine and one atom on MAA according to eq 2 using a 2.0 kcal/mol/Å^2 force constant (k_r) and the equilibrium distance (d_0) for a given umbrella sampling window.

$$V'(d) = 0.5k_r(d - d_0)^2 \quad (2)$$

Finally, each of the final PMFs presented was the result of the analysis of a total of 17 individual simulations, each performed at a given functional monomer−template atomic separation distance (d_0) varying from 10.3 to 1.9 Å. Every window distance studied consisted of 100 ps of equilibration followed by a 400 ps production phase in which variations in the atomic separation distance of MAA-bupivacaine were collected (totally 6800 ps). A total of 20 000 configurations was collected for each window.

The 1:1 complex formation in chloroform was studied using three different starting configurations of monomer and template (additionally restraining the *CO-MH*, *AN-MH*, and *AH-MH* bupivacaine-MAA atomic distances, see Chart 1) to improve the quality of the statistical analysis.

Variation around the restrained separation distances obtained from the production phases studied were analyzed using the weighted histogram method (WHAM)[29,30] as implemented by Grossfield,[31] and the generated PMF was finally corrected for entropy volume effects according to eq 3 (see Table S4 and Figure S8 (Supporting Information) for further details regarding this analysis).

$$\mathrm{PMF}_{\mathrm{corr}} = \mathrm{PMF} + \Delta S_{\mathrm{vol}} = \mathrm{PMF} + k_B T \ln\left(\frac{V_{\mathrm{shell}}}{V_0}\right) \quad (3)$$

In this expression the Boltzmann's constant (k_B) is expressed as 0.00198 kcal/mol/K, T is the absolute temperature at which the simulations were conducted, and V_0 is an arbitrary volume used in the calculations. The spherical shell volume (V_{shell}) for each binned distance (r) was calculated using the bin width, δr, according to eq 4.

$$V_{\mathrm{shell}} = 4\pi \int_{r-0.5\delta r}^{r+0.5\delta r} r^2 \, \mathrm{d}r \quad (4)$$

Results and Discussion

Complexity of the Prepolymerization Mixture. Through a series of previous investigations we proposed a model to describe the molecular basis for recognition in bupivacaine molecularly imprinted polymers (MIPs). A combination of NMR and radioligand binding studies was used to propose modes for template complexation in the prepolymerization mixture.[17] These experiments indicated formation of MAA-bupivacaine complexes with apparent equilibrium association constants (K_A) of the order of 10^1 M^{-1}; however, the results present only an average picture of the complexation of the template. The number and distribution of modes of complexation is not apparent from these studies. Moreover, recent work has demonstrated that potentially all components in a prepolymerization mixture can contribute to template complexation.[12] Accordingly, we believe that a holistic treatment of the prepolymerization mixture is necessary in order to characterize the factors underlying the formation of template selective sites in resultant polymers and to explain the recognition site heterogeneity exhibited by these materials.

MD simulations have been used for the study of macroscopic properties of molecular systems including, e.g., the dynamic behavior of proteins,[32,33] DNA,[34] membranes,[35] and organic polymers.[36] To investigate the nature of template complexation, theoretical treatments using molecular dynamics (MD) were conducted. In order to highlight the importance of studying the complete MIP prepolymerization mixture, two separate systems were designed, simulated, and analyzed using the MD method: first, a system identical in composition to that used for polymerization (**P**), which included multiple template structures (bupivacaine), functional monomer (MAA), cross-linker (EDMA), initiator (AIBN), and explicit solvent (chloroform). MAA and template were used in their neutral forms, as the nature of their interaction in chloroform is not clear. Moreover, the relative strength of the interactions between the two species is reflected in the lifetimes of the various interactions. A second, simplified, prepolymerization system (**SP**) was also studied in which cross-linker and initiator were omitted.

After equilibration of the two systems, 5 ns MD simulation production runs were conducted. From the resultant trajectories, the average spatial distribution of MAA around bupivacaine was extracted using radial distribution functions (RDFs). In the case of **SP**, RDFs revealed that the density of MAA in the vicinity (<3.0 Å) of the template was higher than the average number density, Chart 1 and Figure 1. Interestingly, evidence for the involvement of a second MAA in template complexation was observed at distances of ≥4.5 Å from the bupivacaine atomic reference point (the carbonyl oxygen). Since hydrogen bonding

(29) Kumar, S.; Bouzida, D.; Swendsen, R. H.; Kollman, P. A.; Rosenberg, J. M. *J. Comput. Chem.* **1992**, *13*, 1011–1021.
(30) Kumar, S.; Rosenberg, J. M.; Bouzida, D.; Swendsen, R. H.; Kollman, P. A. *J. Comput. Chem.* **1995**, *16*, 1339–1350.
(31) Grossfield, A. http://membrane.urmc.rochester.edu/Software/WHAM/WHAM.html (accessed Oct 2008).
(32) Soares, C. M.; Martel, P. J.; Mendes, J.; Carrondo, M. A. *Biophys. J.* **1998**, *74*, 1708–1721.
(33) Díaz, N.; Súarez, D.; Sordo, T. L.; Merz, J. K. M. *J. Med. Chem.* **2001**, *44*, 250–260.
(34) Young, M. A.; Ravishanker, G.; Beveridge, D. L. *Biophys. J.* **1997**, *73*, 2313–2336.
(35) Marrink, S.-J.; Berkowitz, M.; Berendsen, H. J. C. *Langmuir* **1993**, *9*, 3122–3131.
(36) Pant, P. V. K.; Boyd, R. H. *Macromolecules* **1993**, *26*, 679–686.

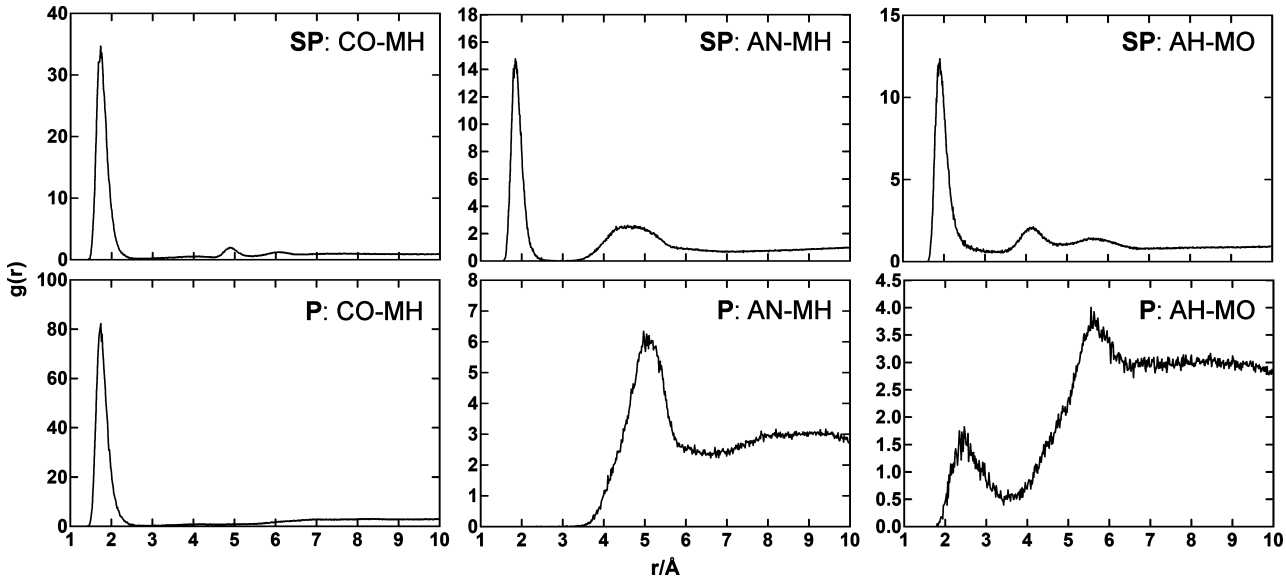

Figure 1. RDFs showing probabilities of finding atomic densities of MAA at different separation distances from the bupivacaine functional groups in the simplified (**SP**) and all-component (**P**) prepolymerization mixtures. See Chart 1 for a description of the investigated atom pairs.

interactions depend on both the distance and the orientation between hydrogen bond accepting and donating groups, all interactions were extracted from the trajectory data using a bond cutoff distance of 3.0 Å and an angle cutoff of 60°.

The average MAA-bupivacaine complex survival (in percent of total simulation time) and hydrogen bond lifetimes of the **SP** system was examined: 47.8% and $\tau = 13.2 \pm 7.1$ ps for the *MH-CO*, 27.4% and $\tau = 5.7 \pm 2.4$ ps for the *MH-AN* and finally 17.9% and $\tau = 1.8 \pm 0.8$ ps for the *MO-AH* interaction. The observed average hydrogen bond lifetime for the interaction between MAA and the *CO* functionality of bupivacaine is of the same order of magnitude as observed for the interaction of methanol and *N*-methylacetamide (NMA) as studied by time-resolved 2D IR spectroscopy and MD ($\tau = 10-15$ ps).[37]

Analysis of the complete prepolymerization system, **P**, was performed similarly using RDFs and hydrogen bonding analysis. Significant differences were observed between the results from **P** and those from the simplified **SP** case. Although the significant *CO-MH* atomic contact was also present in this system, with complex survival and lifetime of 34.1% and $\tau = 11.9 \pm 7.5$ ps, the interaction of MAA with *AN* and *AH* of bupivacaine was seen to be significantly weakened and the atomic distributions were shifted toward longer separation distances, Figure 1 and Table S3 (Supporting Information). Furthermore, the presence of an internal hydrogen bond between the amide proton and amine of the template is also observed, in both the presence and the absence of cross-linker. Interestingly, the average lifetime of this interaction is less than for the stronger functional monomer−template interactions.

NMR titration studies of prepolymerization mixtures indicate significant interaction between monomer and template in both complete ($K_A = 6.4 \pm 2.4$ M^{-1}, Figure S5 (Supporting Information)) and simplified (in the absence of cross-linker and initiator ($K_A = 9.8 \pm 2.3$ M^{-1}) systems (Figures S1 and S2 (Supporting Information)). Moreover, the asymmetry evident in the continuous variation study (Job plots, Figures S3 and S4 (Supporting Information)) point to the presence of higher order complexes. This is in agreement with previous studies in toluene.[16] In an attempt to quantify the average number of MAA molecules present at a close separation distance from the bupivacaine reference positions, RDFs were integrated (up to the distance cutoff value, R_{cut}(Å)) and radial shell numbers, $n_{ij}(r)$, were determined (Table S5 (Supporting Information)). This revealed that on average ∼2 molecules of MAA were found in close contact with each bupivacaine molecule in **SP**. Importantly, for the **P** system which includes EDMA and AIBN, the MAA density in close proximity (≤6.5 Å, see Table S5 (Supporting Information)) to the bupivacaine reference points was found to decrease to ∼1 molecule. The influence of cross-linker on the extent of MAA-bupivacaine complexation is significant. In the presence of EDMA the carbonyl functionalities of the cross-linker interact with the amide proton of the template, hindering access to the amine. As observed in the grid analysis (see later), the weaker nature of this interaction, relative to that of MAA with the amine, appears to be compensated for by the significant excess of cross-linker in the system, 12 and 110 carbonyl groups per template, for MAA and EDMA, respectively. The diversity of cross-linker interaction with template can therefore be seen to influence the heterogeneity of the template complexes formed in the prepolymerization mixture. Accordingly, this result alone highlights the importance of an all-component treatment of MIP prepolymerization mixtures when making predictions concerning the nature of monomer −template complexation.

To further characterize the nature of the noncovalent MAA-bupivacaine complexes formed in chloroform and to allow correlation with NMR data, a series of simulations were performed to obtain free energy profiles through the calculation of potentials of mean force (PMFs) for MAA-bupivacaine complexes of 1:1 stoichiometry. Generation of PMFs enable both the changes in free energy, ΔG_{Bind}, associated with the binding events to be determined and the accessibility of the respective functional groups of bupivacaine to MAA to be investigated, Figure S9 (Supporting Information). PMF analyses demonstrated that the *CO* functionality of bupivacaine was the most accessible to MAA. Interestingly, in PMF analyses binding of MAA to the *CO* functionality of bupivacaine was clearly

(37) Woutersen, S.; Mu, Y.; Stock, G.; Hamm, P. *Chem. Phys.* **2001**, *266*, 137147.s.

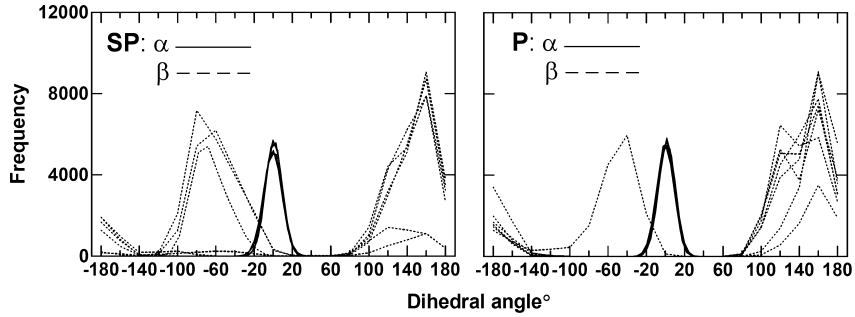

Figure 2. Variations in the α (solid lines) and β (dashed lines) dihedral angles (described in Chart 2) for the each of the seven bupivacaine molecules present in the **SP** and **P** model mixtures.

the most dominant interaction observed in the ensemble of MAA-bupivacaine complexes formed. The strengths of these complexes were dependent upon the relative orientation of MAA and bupivacaine with the weakest binding of $\Delta G_{\text{Bind}} = -1.14$ kcal/mol ($K_A = 7.2\ M^{-1}$), medium binding of -2.43 kcal/mol ($K_A = 64.7\ M^{-1}$), and the strongest interaction observed of -4.30 kcal/mol ($K_A = 1618\ M^{-1}$). These data highlight the importance of MAA's interaction with *CO*, something which is not immediately apparent from NMR studies. Accordingly, this type of theoretical treatment together with the NMR data provides a more complete picture of the events underlying template complexation.

To determine the fate of the complexes observed in the prepolymerization mixture, the polymerization process was followed by ^{1}H NMR. Importantly, the shifts induced by the MAA-template interactions were sustained even 45 min into the polymerization when gelation was quite apparent (Figure S7 (Supporting Information)).

On the Origin of MIP Recognition Site Heterogeneity. It is evident from the results of the NMR and MD studies of the full (**P**) and simplified (**SP**) prepolymerization systems that all components should be taken into consideration when describing the microenvironment of the template. As the presence of EDMA and AIBN clearly had an impact on the distribution of MAA around bupivacaine, it was deemed necessary to examine the role of all possible component configurations. EDMA-bupivacaine RDFs, illustrating the distribution of EDMA oxygens around atomic reference positions on bupivacaine, revealed ordered shells of EDMA in close proximity to the template (≤5 Å, Figure S10 (Supporting Information)).

Compared to MAA-bupivacaine RDFs, EDMA-bupivacaine RDFs are typically broader which we suggest reflects both the weak nature of EDMA's interaction with the template and the flexibility inherent to EDMA. Furthermore, EDMA was observed to cluster around the *CO* and *AN* sites of bupivacaine. This observation was based on the fact that the ester oxygens of EDMA (*EO1* and *EO2*) were closer to the *CO* functionality of bupivacaine than the ester group carbonyl oxygens (*EO* and *EO3*) which were found to be more strongly associated with the *AN* functionality. From these observations we conclude that despite being weak, EDMA forms interactions with bupivacaine. We suggest this to be a significant factor in the formation of shape-selective template recognition sites in the resultant MIP. This was further supported by ^{1}H NMR titration studies which showed that EDMA induced small changes in the chemical shifts of selected bupivacaine protons (Figure S6 (Supporting Information)).

A further issue addressed was the influence of EDMA on template conformation during complexation. Variation in the α and β dihedral angles of bupivacaine (explained in Chart 2) for each of the seven bupivacaine molecules present in each simulated mixture was examined. For **SP**, the conformations of bupivacaine were found to be represented by an α dihedral angle of 0° and varying angles of β of either $-60°$ or 160°, Figure 3. This corresponds to conformations in which the dimethyl phenyl and *N*-butyl alkyl side chain groups are either located in the same plane ($\beta = -60°$) or out of the plane ($\beta = 160°$). These conformations of bupivacaine were estimated to be present in equal amounts in **SP**. In the case of **P** the β dihedral angle population of bupivacaine was restricted to $\beta = 160°$ (the distribution of template conformations can also be seen in the grid density representations, e.g., Figure 3).

We conclude that the change in the population of bupivacaine conformations observed in **P** (Figure 2) is driven by changes in the local microenvironment due to the presence of EDMA. The induced change in the conformation of bupivacaine supports the hypothesis for the presence of a network of EDMA molecules in near proximity to bupivacaine. An extrapolation of this conclusion may explain why more functionalized cross-linking agents can be successfully used to fabricate ligand-selective MIPs, as in the case of the OMNI-MIP work by Spivak and colleagues.[38,39]

Recently Jitera and Kollman[26] presented a method in which the position of one atom or structure, e.g., the monomer, is tracked relative to a second, e.g., the template, as the simulation proceeds. Results are visualized as 3-dimensional grid densities. Visualization of the different atomic grid density distributions of MAA with respect to each bupivacaine molecule present in **P**, Figure 3, demonstrated the diversity of template complexation (for the corresponding distribution in **SP** see Figure S15 (Supporting Information)). The RDF analyses described earlier reflect the average distribution of the functional monomer around the template, though here the contributing populations of interactions and their geometries are made evident using this technique. Importantly, the use of multiple template structures revealed a variability in the degree of complexation by the functional monomer.

Since all interaction events occurring in the prepolymerization solution will in principle influence the template recognition characteristics of the resultant MIP, the contribution of other components must also be considered to describe the origin of recognition site heterogeneity demonstrated by MIPs. Template self-association has previously been demonstrated to influence

(38) Sibrian-Vazquez, M.; Spivak, D. A. *J. Am. Chem. Soc.* **2005**, *126* (25), 7827–7833.
(39) Sibrian-Vazquez, M.; Spivak, D. A. *Macromolecules* **2003**, *36* (14), 5105–5113.

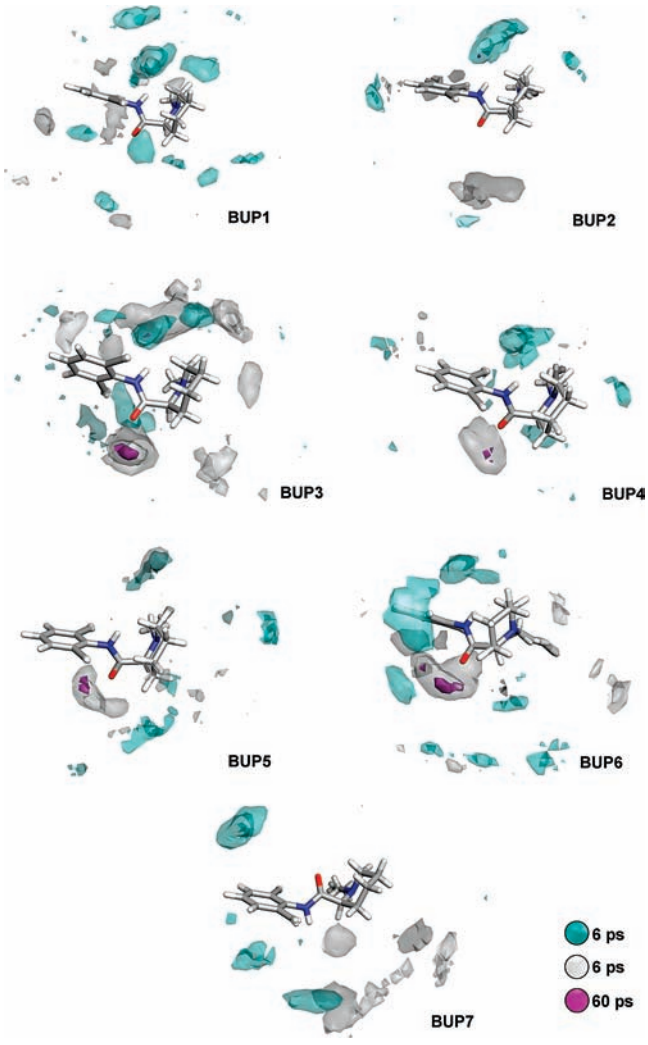

Figure 3. 3D grid density representations of the series of prepolymerization complexes observed for **P**. Densities describe the probability and associated lifetimes for finding the *MH* atom of MAA (gray) or the *EO* atom of EDMA (green) around the seven molecules of bupivacaine present. Higher contour values for both MAA and EDMA are presented in purple. See Chart 1 for a description of the atoms studied.

polymer performance.[9−12] Both complete and simplified systems were investigated to determine if evidence for bupivacaine-bupivacaine interactions was present. While bupivacaine molecules in **SP** were found to be randomly distributed, the presence of initiator and cross-linker induced a more ordered bupivacaine-bupivacaine distribution in **P** (Figure S12 (Supporting Information)). This behavior was explained on the basis of competition from EDMA for interaction with bupivacaine structures, thereby restricting the flexibility and mobility of the template (see later). Additionally, the sharpness of the first peak in the bupivacaine-bupivacaine RDF and subsequent results from hydrogen bond analysis (Table S3 (Supporting Information)) show that the limited observed dimerization of bupivacaine (<7%) is mainly driven by the formation of hydrogen bonds, preferably between the *CO-AH* functionalities. From these analyses, however, we believe that the self-association of bupivacaine observed in the case of **P** is insufficient to significantly influence the recognition site population of the MIP.

Monomer−monomer interactions provided a second focus. MAA and the functional monomer analogue AcOH self-associate through the formation of either one or two hydrogen bonds with K_A of 1200 M^{-1} for MAA[40] and 2487 M^{-1} for AcOH.[41] The strength of MAA dimerization relative to the predicted strength for MAA-bupivacaine association (from PMF calculations, values ranging from 7.2 to 1618 M^{-1}) reflects the competitive nature of the various interactions present in the prepolymerization mixture, which is also reflected in the presence of both free and self-associated MAA. The importance of monomer−template interactions in determining the ultimate recognition behavior of the polymer and even in terms of recognition site heterogeneity is reflected in the success that has been obtained through the use of very stable interactions, e.g., guanidine-carboxyl and urea-phosphonate interactions.[42]

The dimerization of MAA (Figure S13 (Supporting Information)) was investigated for both **SP** and **P** solutions. In both cases, the *MC-MC* RDFs exhibited two closely separated peaks centered at 3.9 and 4.2 Å, respectively, and an additional atomic distribution shell at ∼6 Å. The density maxima at 3.9 and 4.2 Å correspond to dimers of MAA interacting via either one or two hydrogen bonds, whereas the second, broader peak may be attributed to MAA present in close vicinity to the observed pairs of MAA. Interestingly, the ratio between these two fractions in the RDFs decreases from 6:1 in the **SP** mixture to 3:1 for the **P** mixture, indicating that MAA dimerization is less favored when EDMA and AIBN are present.

The behavior of the porogen in the prepolymerization was also examined. Although it is generally accepted that a nonpolar solvent competes less with functional monomers for polar interaction points on a template structure, its nonspecific interactions with polymer components will have a strong influence on final MIP performance by affecting, e.g., polymer surface area and pore volumes. Interestingly, the chloroform-bupivacaine distributions (Figures S14, S16, and S17 (Supporting Information)) exhibited very similar profiles for both **SP** and **P**. Analysis showed that chloroform is predominantly located around the nonpolar parts of bupivacaine such as the dimethylphenyl and *N*-butyl groups. Integration of the sharpest, first, peak in the chloroform RDFs resulted in an average radial shell number of ∼1 molecule of chloroform present within a radius of 4 Å from the *CO* position of bupivacaine in **SP**. This value for the interaction of chloroform-bupivacaine decreased to ∼0.5 molecule in the all-component prepolymerization solution, **P**. This decrease in the density of chloroform around the dimethylphenyl group of bupivacaine was attributed to competition from EDMA.

Finally, the distribution of AIBN relative to bupivacaine demonstrated no evidence of interaction (Figures S11 and S18 (Supporting Information)). Accordingly, this result suggests that for the system studied here, the initiator does not perturb monomer−template complexation. Collectively, the diversity of template complexes and the competition for interaction between the various species present provide a detailed description of the prepolymerization mixture. The involvement of, in particular, functional monomer in interactions with entities other than template results in a spatial distribution of carboxyl groups in the polymer that plays a significant role in the observed heterogeneity. This effect is exacerbated by template confor-

(40) Ansell, R. J.; Kuah, K. L. *Analyst* **2005**, *130*, 179–187.
(41) Chocholousová, J.; Vacek, J.; Hobza, P. *J. Phys. Chem. A* **2003**, *107*, 3086–3092.
(42) (a) Emgenbroich, M.; Borelli, C.; Shinde, S.; Lazraq, I.; Vilela, F.; Hall, A. J.; Oxelbark, J.; De Lorenzi, E.; Courtois, J.; Simanova, A.; Verhage, J.; Irgum, K.; Karim, K.; Sellergren, B. *Chem.−Eur. J.* **2008**, *14*, 9516–9529. (b) Wulff, G.; Schönfeld, R. *Adv. Mater.* **1998**, *10*, 957–959. (c) Wulff, G.; Knorr, K. *Bioseparation* **2002**, *10*, 257–276.

mational variability. With support from NMR studies of the initial stages of polymer gelation, we propose that this heterogeneity is the origin of the recognition site distribution observed in this and other MIP systems. To verify the interactions observed in the MD simulations, polymers (imprinted, MIP, and nonimprinted, REF) corresponding to **P** were synthesized and characterized.

Previous attempts have been made to quantify the heterogeneity of a MIP by using mathematical treatments of binding data, e.g., fitting to Freundlich isotherms. Shimizu et al.[43] proposed that differences in the binding site heterogeneity and even imprinting effects can be described by comparison of m values, a measure of binding site heterogeniety. Interestingly, they also demonstrated that the value of m was found to be strongly dependent upon the concentration of MIP used in the binding experiments employed. To avoid this complication we utilized polymer-titration studies where a constant amount of bupivacaine was incubated with various concentrations of polymer. The radioligand binding studies revealed that the MIP displayed an approximately 3-fold greater binding capacity than REF, based upon PC_{50} values (MIP = 0.9 mg/mL and REF = 2.5 mg/mL). When normalized to account for differences in BET-surface area the imprinting effect is even more pronounced: MIP 80.4 pmol/m^2 and REF 12.0 pmol/m^2 (see Figure S19 (Supporting Information)).

At the suggestion of a referee, the role of the α,β-unsaturation of the functional monomer was investigated. NMR and MD studies (Figure S20 and S21 and Table S6 (Supporting Information)) revealed that MAA binds a factor of 2 more strongly to template than isobutyric acid. Thus, the presence of the double bond in MAA affects the electronic distribution, as reflected in the pK_a values of the acids (MAA = 4.65 and isobutyric acid = 4.83).[44] Both the higher pK_a and the lack of $\pi-\pi$-type interactions may contribute to the overall weaker interaction of the saturated functional monomer analogue with template.

Conclusions

In this paper, we studied the origin of binding site heterogeneity in a molecularly imprinted methacrylic acid−ethylene dimethacrylate copolymer. Results from a series of experimental ^{1}H NMR spectroscopic and theoretical classical molecular dynamics simulations are used to argue that the heterogeneity originates from the presence of an ensemble of MAA-EDMA-bupivacaine complexes present in the prepolymerization stage. This work provides the first realistic view of the nature of the prepolymerization mixture and accounts for self-association events between template and monomer molecules, multiple complexation modes, the role of porogen, and dynamic processes. The role of cross-linker during the formation of recognition sites is also most evident. We believe that studying the nature of the complexes formed in solution may be used to explain the selectivity (or lack thereof) of a MIP. The system studied has been validated through polymer synthesis and radioligand binding and BET studies.

Other strategies have been developed which offer potential for the template-driven synthesis of recognition materials with greater fidelity than generally available today, such as dynamic combinatorial chemistry,[45] where reversible covalent interactions are used to steer toward greater numbers of the thermodynamically favored monomer−template interactions. In the case of molecular imprinting, the polymerization step is not under thermodynamic control, though efforts have been made with disulfide cross-linked polymers.[46] Herein lies both the inherent beauties and weaknesses of both strategies. The fact that the polymerization process is under kinetic control makes the nature of template complexation of paramount importance for dictating the recognition site distribution in resultant polymers. This is reflected in the gains in homogeneity obtained with systems where stoichiometric noncovalent interactions are used.[42]

The computational modeling of various aspects of the molecular imprinting process has gained increasing prominence over recent years,[47] and recently, stochastic treatments have been employed to describe MIP behavior.[48] This first full system study demonstrates that theoretical treatments of molecular-imprinting systems must include all interaction types, e.g., template−template, solvent−template, monomer−monomer, and molecular conformational effects, etc., in order to adequately describe a system. Finally, the complexity of the intermolecular interactions present in the prepolymerization mixture results in an ensemble of complexes which in turn manifest themselves as site heterogeneity in the resultant polymers. The strategy described here, a combination of theoretical and NMR studies, should provide a sound basis for the development of tools for rational MIP design.

Acknowledgment. The financial support of the Swedish Research Council (V.R.), the Carl Trygger Foundation, the Swedish Knowledge Foundation (K.K.S.), and the University of Kalmar is most gratefully acknowledged.

Supporting Information Available: ^{1}H NMR studies (titrations, continuous variation, polymerization), molecular dynamics studies (equilibrium and production phase data, potentials of mean force calculations, RDF and grid analyses), and polymer titration data. This material is available free of charge via the Internet at http://pubs.acs.org.

JA902087T

(43) Rushton, G. T.; Karns, C. L.; Shimizu, K. D. *Anal. Chim. Acta* **2005**, *528*, 107–113.
(44) Dong, H.; Du, H.; Qian, X. *J. Phys. Chem. A* **2008**, *112*, 12687–12694.
(45) (a) Lehn, J. *Science* **2002**, *295*, 2400–2403. (b) Lehn, J. *Proc. Nat. Acad. Sci.* **2002**, *99*, 4763–4768. (c) Rowan, S. J.; Cantrill, S. J.; Cousins, G. R. L.; Sanders, J. K. M.; Stoddart, J. F. *Angew. Chem., Int. Ed.* **2002**, *41*, 898–952.
(46) Mukawa, T.; Goto, T.; Takeuchi, T. *Analyst* **2002**, *127*, 1407–1409.
(47) Nicholls, I. A.; Andersson, H. S.; Charlton, C.; Henschel, H.; Karlsson, B. C. G.; Karlsson, J. G.; O'Mahony, J.; Rosengren, A. M.; Rosengren, K. J.; Wikman, S. *Biosens. Bioelectron.* **2009**; doi 10.1016/j.bios.2009.03.038.
(48) Wu, X.; Carroll, W. R.; Shimizu, K. *Chem. Mater.* **2008**, *20* (13), 4335–4346.